Accurate, Efficient Quantification of Uncertainty for Flow in Heterogeneous Reservoirs Using the KLME Approach

Zhiming Lu, Los Alamos Natl. Laboratory, and **Dongxiao Zhang,** SPE, U. of Oklahoma

Summary

Accurate modeling of flow in oil/gas reservoirs requires a detailed description of reservoir properties such as permeability and porosity. However, such reservoirs are inherently heterogeneous and exhibit a high degree of spatial variability in medium properties. Significant spatial heterogeneity and a limited number of measurements lead to uncertainty in characterization of reservoir properties and thus to uncertainty in predicting flow in the reservoirs. As a result, the equations that govern flow in such reservoirs are treated as stochastic partial differential equations. The current industrial practice is to tackle the problem of uncertainty quantification by Monte Carlo simulations (MCS). This entails generating a large number of equally likely random realizations of the reservoir fields with parameter statistics derived from sampling, solving deterministic flow equations for each realization, and post-processing the results over all realizations to obtain sample moments of the solution. This approach has the advantages of applying to a broad range of both linear and nonlinear flow problems, but it has a number of potential drawbacks. To properly resolve high-frequency space-time fluctuations in random parameters, it is necessary to employ fine numerical grids in space-time. Therefore, the computational effort for each realization is usually large, especially for large-scale reservoirs. As a result, a detailed assessment of the uncertainty associated with flow-performance predictions is rarely performed.

In this work, we develop an accurate yet efficient approach for solving flow problems in heterogeneous reservoirs. We do so by obtaining higher-order solutions of the prediction and the associated uncertainty of reservoir flow quantities using the moment-equation approach based on Karhunen-Loéve decomposition (KLME). The KLME approach is developed on the basis of the Karhunen-Loéve (KL) decomposition, polynomial expansion, and perturbation methods. We conduct MCS and compare these results against different orders of approximations from the KLME method. The 3D computational examples demonstrate that this KLME method is computationally more efficient than both Monte Carlo simulations and the conventional moment-equation method. The KLME approach allows us to evaluate higher-order terms that are needed for highly heterogeneous reservoirs. In addition, like the Monte Carlo method, the KLME approach can be implemented with existing simulators in a straightforward manner, and they are inherently parallel. The efficiency of the KLME method makes it possible to simulate fluid flow in large-scale heterogeneous reservoirs.

Introduction

Owing to the heterogeneity of geological formations and the incomplete knowledge of medium properties, the medium properties may be treated as random functions, and the equations describing flow and transport in these formations become stochastic. Stochastic approaches to flow and transport in heterogeneous porous media have been extensively studied in the last 2 decades, and many stochastic models have been developed (Dagan 1989; Gelhar 1993; Zhang 2002). Two commonly used approaches for solving stochastic equations are MCS and the moment-equation method. A major disadvantage of the Monte Carlo method, among others, is the requirement for large computational efforts. An alternative to MCS is an approach based on moment equations, the essence of which is to derive a system of deterministic partial differential equations governing the statistical moments [usually the first two moments (i.e., mean and covariance)], and then solve them analytically or numerically. However, the computational cost for the conventional moment method is still high. In computing the pressure-head covariance up to first order in σ_Y^2, the variability of the log hydraulic conductivity of the heterogeneous reservoir, $Y=\ln[K_s(\mathbf{x})]$, one needs to solve sets of deterministic linear algebraic equations on a grid of N nodes for approximately $2N$ times: N times for solving the cross-covariance between the pressure head and the log hydraulic conductivity C_{Yh} and approximately N time for the pressure head covariance C_h. Including high-order terms is possible, but it will increase the computational effort dramatically.

To alleviate the computational burden, Zhang and Lu (2003) developed a new approach that combines KLME and perturbation methods. Specifically, using the new approach, with a much lower computational cost, they were able to evaluate the mean pressure head and the mean flux up to fourth order in σ_Y and the pressure-head and flux variances to the third order in σ_Y^2. Yang et al. (2004) applied this method to simulating water flow in unsaturated soils, in which the permeability depends on the pressure head in a nonlinear manner. Lu and Zhang (2004a) developed a conditional KLME method to incorporate permeability measurements in the reservoirs. Chen et al. (2005) extended the KLME method to simulate two-phase flow problems (water and oil phases) in which the constitutive relation between the relative permeability and the capillary pressure follows an exponential model. All these studies are limited to steady-state flow in 2D domains. In this study, we extend the KLME approach to transient fluid flow in the 3D space, compare the KLME approach with both the Monte Carlo method and the conventional moment-equation method (Zhang 2002; Li et al. 2003; Li and Tchelepi 2003), and demonstrate the applicability of this approach to simulating flow in large-scale heterogeneous reservoirs.

Statement of Problem

We consider transient fluid flow in heterogeneous reservoirs satisfying the following equation:

$$\nabla \cdot [K_s(\mathbf{x})\nabla h(\mathbf{x}, t)] + g(\mathbf{x}, t) = S_s \frac{\partial h(\mathbf{x}, t)}{\partial t}, \quad \ldots\ldots\ldots\ldots\ldots (1)$$

subject to initial and boundary conditions

$$h(\mathbf{x}, 0) = H_0(\mathbf{x}), \qquad \mathbf{x} \in D, \ldots\ldots\ldots\ldots\ldots (2)$$

$$h(\mathbf{x}, t) = H(\mathbf{x}, t), \qquad \mathbf{x} \in \Gamma_D, \ldots\ldots\ldots\ldots\ldots (3)$$

$$K_s(\mathbf{x})\nabla h(\mathbf{x}, t) \cdot \mathbf{n}(\mathbf{x}) = -Q(\mathbf{x}, t), \qquad \mathbf{x} \in \Gamma_N, \ldots\ldots\ldots\ldots\ldots (4)$$

where $h(\mathbf{x}, t)$ is the hydraulic pressure head, $K_s(\mathbf{x})$ is the hydraulic conductivity, $g(\mathbf{x}, t)$ is the source/sink term, S_s is the specific storage, $H_0(\mathbf{x})$ is the initial pressure head in the flow domain D, $H(\mathbf{x}, t)$ is the prescribed pressure head on the Dirichlet boundary segments Γ_D, $Q(\mathbf{x}, t)$ is the flux across Neumann boundary seg-

Copyright © 2006 Society of Petroleum Engineers

This paper (SPE 93452) was first presented at the 2005 SPE Reservoir Simulation Symposium, Houston, 31 January–2 February, and revised for publication. Original manuscript received for review 20 June 2005. Revised manuscript received 27 December 2005. Paper peer approved 3 January 2006.

ments Γ_N, $\mathbf{n}$ is an outward unit vector normal to the boundary $\Gamma = \Gamma_D \cup \Gamma_N$, $\mathbf{x} = (x_1, x_2, x_3)^T$ is the Cartesian coordinate, and t is the time. In this study, we consider K_s as a random function, while all initial and boundary conditions as well as the specific storage are assumed to be deterministic. Our aim is to estimate efficiently the mean pressure head and its associated uncertainty. The moments of the flux can be obtained on the basis of the pressure-head moments (Lu and Zhang 2004a), and the moments of the well flow rates can also be obtained with the pressure statistics through the Peaceman well models.

Karhunen-Loève Decomposition

The Karhunen-Loève decomposition of a log hydraulic conductivity field $Y(\mathbf{x}) = \ln [K_s(\mathbf{x})]$ can be found in the literature (Zhang and Lu 2004; Ghanem and Spanos 1991; Roy and Grilli 1997; Lu and Zhang 2004b). The basic idea is to decompose the covariance function $C_Y(\mathbf{x}, \mathbf{y}) = \langle Y'(\mathbf{x})Y'(\mathbf{y})\rangle$ into $C_Y(\mathbf{x}, \mathbf{y}) = \sum \lambda_n f_n(\mathbf{x}) f_n(\mathbf{y})$, where λ_n and f_n are eigenvalues and orthogonal deterministic eigenfunctions, respectively, and can be solved from the following Fredholm equation:

$$\int_D C_Y(\mathbf{x}, \mathbf{y}) f(\mathbf{x}) d\mathbf{x} = \lambda f(\mathbf{y}). \quad (5)$$

The mean-removed stochastic process $Y'(\boldsymbol{x})$ can then be expanded in terms of λ_n and f_n as

$$Y'(\mathbf{x}) = \sum_{n=1}^{\infty} \xi_n \sqrt{\lambda_n} f_n(\mathbf{x}), \quad (6)$$

where ξ_n are orthogonal standard Gaussian random variables (i.e., $\langle \xi_n \rangle = 0$ and $\langle \xi_i \xi_j \rangle = \delta_{ij}$) if Y is normally distributed. It has been shown that the KL expansion is of mean-square convergence and may be well approximated with a finite summation. If the direct measurements of the hydraulic conductivity field are available, one can decompose the conditional field using an expression similar to Eq. 6 with the conditional eigenvalues $\lambda_n^{(c)}$ and eigenfunctions $f_n^{(c)}$ (Lu and Zhang 2004a), and the mathematical derivation for the KL-based moment equations presented in the next section is still valid.

Squaring both sides of Eq. 6, taking the ensemble mean, and integrating the resulting equation yields $\sum \lambda_n = \sigma_Y^2 V$, where V is the volume of the simulation domain D. In addition, the series of eigenvalues are nonincreasing, and the characteristic scale of f_n decreases as n increases (Zhang and Lu 2004). Therefore, the terms in the series in Eq. 6 represent fluctuations of decreasing magnitude and scale as n increases. This allows us to truncate the expansion in Eq. 6 by keeping only a finite number of terms.

Eq. 6 provides an alternative way for generating random fields. Once eigenvalues λ_n and their corresponding eigenfunctions f_n are found, a realization can be computed simply by independently sampling a certain number of values ξ_n from the standard Gaussian distribution $N(0, 1)$, and then approximating $Y'(\mathbf{x})$ in Eq. 6 by $\sum_1^M \xi_n \sqrt{\lambda_n} f_n$, where M is the number of terms needed to reproduce the Y variability with a given accuracy. The number M depends on the ratio of the correlation length to the dimension of the domain. Detailed discussion can be found in Zhang and Lu (2004).

Because the eigenvalues $\sqrt{\lambda_n}$ and their corresponding eigenfunctions f_n always come together in the derivation given in the following section, we define new functions $\tilde{f}_n = \sqrt{\lambda_n} f_n$ and the tilde over f_n is then dropped for simplicity.

KLME

We decompose the log hydraulic conductivity as $Y(\mathbf{x}) = \ln K_s(\mathbf{x}) = \langle Y(\mathbf{x})\rangle + Y'(\mathbf{x})$ and the pressure head as $h(\boldsymbol{x}, t) = h^{(0)} + h^{(1)} + h^{(2)} + \cdots$. In the series, the order of each term is with respect to σ_Y, the standard deviation of Y. Upon substituting the expansions of $h(\mathbf{x}, t)$ and Y into Eqs. 1 through 4, and collecting terms at separate order, one obtains the following equations that govern the pressure head at different orders in terms of σ_Y (see Zhang 2002):

$$\nabla \cdot [K_G(\mathbf{x}) \nabla h^{(0)}(\mathbf{x}, t)] + g(\mathbf{x}, t) = S_s \frac{\partial h^{(0)}(\mathbf{x}, t)}{\partial t}, \quad (7)$$

subject to initial and boundary conditions:

$$h^{(0)}(\mathbf{x}, 0) = H_0(\mathbf{x}), \qquad \mathbf{x} \in D, \quad (8)$$

$$h^{(0)}(\mathbf{x}, t) = H(\mathbf{x}, t), \qquad \mathbf{x} \in \Gamma_D, \quad (9)$$

$$K_G(\mathbf{x}) \nabla h^{(0)}(\mathbf{x}, t) \cdot \mathbf{n}(\mathbf{x}) = -Q(\mathbf{x}, t), \qquad \mathbf{x} \in \Gamma_N, \quad (10)$$

and for m≥1,

$$\nabla \cdot [K_G(\mathbf{x}) \nabla h^{(m)}(\mathbf{x}, t)] + g^{(m)}(\mathbf{x}, t) = S_s \frac{\partial h^{(m)}(\mathbf{x}, t)}{\partial t}, \quad (11)$$

subject to initial and boundary conditions:

$$h^{(m)}(\mathbf{x}, 0) = 0, \qquad \mathbf{x} \in D, \quad (12)$$

$$h^{(m)}(\mathbf{x}, t) = 0, \qquad \mathbf{x} \in \Gamma_D, \quad (13)$$

$$K_G(\mathbf{x}) \nabla h^{(m)}(\mathbf{x}, t) \cdot \mathbf{n}(\mathbf{x}) = \frac{(-1)^{m+1}}{m!} [Y'(\mathbf{x})]^m Q(\mathbf{x}, t), \qquad \mathbf{x} \in \Gamma_N, \quad (14)$$

where $K_G(\mathrm{x}) = \exp(\langle Y(\mathrm{x})\rangle)$ is the geometric mean of the hydraulic conductivity, and

$$g^{(m)}(\mathbf{x}, t) = K_G(\mathbf{x}) \nabla Y'(\mathbf{x}) \cdot \nabla h^{(m-1)}(\mathbf{x}, t) + \frac{g(\mathbf{x}, t)}{m!} [-Y'(\mathbf{x})]^m - S_s \sum_{k=1}^{m} \frac{(-1)^k}{m!} [Y'(\mathbf{x})]^k \frac{\partial h^{(m-k)}(\mathbf{x}, t)}{\partial t}. \quad (15)$$

Eqs. 7 through 10 are the governing equations for the 0th-order mean pressure-head solution. In the conventional moment method, the higher-order corrections (usually up to second-order) for the mean pressure head are solved from Eqs. 11 through 15. For example, setting $m = 2$ in Eqs. 11 through 15 and taking the ensemble mean yields the equation with initial and boundary conditions for the second-order pressure-head term $\langle h^{(2)}\rangle$. The latter involves an evaluation of the cross-covariance $C_{Yh} = \langle Y' h^{(1)}\rangle$.

In the conventional-moment method, the equations for the first-order (in terms of σ_Y^2) pressure head covariance $C_h(\mathbf{x}, t; \mathbf{y}, \tau)$ is derived from Eqs. 11 through 15 by setting $m = 1$, multiplying the resulting equations for $h^{(1)}(\mathbf{x}, t)$ by $h^{(1)}(\mathbf{y}, \tau)$, and taking the ensemble mean. It has been shown that the conventional moment method is computationally expensive, especially for large-scale problems. In fact, to solve the pressure-head covariance up to the first order (in σ_Y^2), it is required to solve the sets of linear algebraic equations with N unknowns (N being the number of nodes in the numerical grid) for $2N$ times (Li et al. 2003; Li and Tchelepi 2003): N times for solving the cross-covariance C_{Yh} and N times for the covariance C_h. Solving the pressure-head covariance with higher-order corrections is possible, but the computational effort is very demanding. For instance, solving the pressure-head covariance up to the second order in terms of σ_Y^2 requires solving sets of linear algebraic equations with N unknowns for N^2 times.

In our KLME method, we further assume that $h^{(m)}(\mathbf{x}, t)$ can be expanded in terms of the product of m orthogonal Gaussian random variables (see Appendix). In particular, the first two terms are

$$h^{(1)} = \sum_{i=1}^{\infty} h_i^{(1)} \xi_i, \qquad h^{(2)} = \sum_{i,j=1}^{\infty} h_{ij}^{(2)} \xi_i \xi_j, \quad (16)$$

where $h_i^{(1)}(\mathbf{x}, t)$ and $h_{ij}^{(2)}(\mathbf{x}, t)$ are deterministic coefficients to be determined, and the latter is symmetric with respect to its subscripts i and j. By substituting the decomposition of $Y'(\mathbf{x})$ and $h^{(1)}$ into Eqs. 11 through 15 for $m = 1$, and recalling that the set of random variables ξ_n are orthogonal, we obtain the governing equations for $h_n^{(1)}$:

$$\nabla \cdot [K_G(\mathbf{x})\nabla h_n^{(1)}(\mathbf{x}, t)] + g_n^{(1)}(\mathbf{x}, t) = S_s \frac{\partial h_n^{(1)}(\mathbf{x}, t)}{\partial t}, \quad (17)$$

$$h_n^{(1)}(\mathbf{x}, 0) = 0, \qquad \mathbf{x} \in D, \quad (18)$$

$$h_n^{(1)}(\mathbf{x}, t) = 0, \qquad \mathbf{x} \in \Gamma_D, \quad (19)$$

$$K_G(\mathbf{x})\nabla h_n^{(1)}(\mathbf{x}, t) \cdot \mathbf{n}(\mathbf{x}) = Q(\mathbf{x}, t) f_n(\mathbf{x}), \qquad \mathbf{x} \in \Gamma_N, \quad (20)$$

and

$$g_n^{(1)}(\mathbf{x}, t) = K_G(\mathbf{x})\, \nabla f_n(\mathbf{x}) \cdot \nabla h^{(0)}(\mathbf{x}, t) - g(\mathbf{x}, t) f_n(\mathbf{x}) + S_s f_n(\mathbf{x}) \frac{\partial h^{(0)}(\mathbf{x}, t)}{\partial t}. \quad (21)$$

Similarly, one can derive the equations for $h_{ij}^{(2)}(\mathbf{x}, t)$ as

$$\nabla \cdot [K_G(\mathbf{x})\nabla h_{ij}^{(2)}(\mathbf{x}, t)] + g_{ij}^{(2)}(\mathbf{x}, t) = S_s \frac{\partial h_{ij}^{(2)}(\mathbf{x}, t)}{\partial t}, \quad (22)$$

$$h_{ij}^{(2)}(\mathbf{x}, 0) = 0, \qquad \mathbf{x} \in D, \quad (23)$$

$$h_{ij}^{(2)}(\mathbf{x}, t) = 0, \qquad \mathbf{x} \in \Gamma_D, \quad (24)$$

$$K_G(\mathbf{x})\nabla h_{ij}^{(2)}(\mathbf{x}, t) \cdot \mathbf{n}(\mathbf{x}) = -Q(\mathbf{x}, t) f_i(\mathbf{x}) f_j(\mathbf{x})/2, \qquad \mathbf{x} \in \Gamma_N, \quad (25)$$

where

$$g_{ij}^{(2)}(\mathbf{x}, t) = \frac{K_G(\mathbf{x})}{2}\left[\nabla f_i(\mathbf{x}) \cdot \nabla h_j^{(1)}(\mathbf{x}, t) + f_j(\mathbf{x}) \cdot \nabla h_i^{(1)}(\mathbf{x}, t)\right] + \frac{g(\mathbf{x}, t)}{2} f_i(\mathbf{x}) f_j(\mathbf{x}) - \frac{S_s}{2}\left[f_i(\mathbf{x}) \frac{\partial h_j^{(1)}(\mathbf{x}, t)}{\partial t} + f_j(\mathbf{x}) \frac{\partial h_i^{(1)}(\mathbf{x}, t)}{\partial t} - f_i(\mathbf{x}) f_j(\mathbf{x}) \frac{\partial h^{(0)}(\mathbf{x}, t)}{\partial t}\right]. \quad (26)$$

To maintain the symmetry of the term $h_{ij}^{(2)}(\mathbf{x}, t)$, we have written the term corresponding to $\nabla Y' \cdot \nabla h^{(1)}$ in Eq. 15 as $(\nabla f_i \cdot \nabla h_j^{(1)} + \nabla f_j \cdot \nabla h_i^{(1)})/2$ in Eq. 26. Similar treatment has been done to other terms in Eq. 26. The readers are referred to Zhang and Lu (2004) for details. The more general governing equations for higher-order term $h_{i_1 i_2 \ldots i_m}^{(m)}$ are shown in the Appendix.

As shown in Yang et al. (2004), our expansion would be equivalent to that of Ghanem and Spanos (1991) if both expansions include all higher-order terms. Two expansions differ only in the arrangement of terms. Ghanem and Spanos (1991) expanded the random function in terms of different orders of polynomial chaos, while we expand the random function as different order in terms of its variability, which is physically meaningful. In contrast, the expansion on the polynomial chaos basis does not have a clear physical meaning.

We should emphasize here that the second-order polynomial chaos basis of Ghanem and Spanos (1991), $\{\xi_i\xi_j - \delta_{ij},\ i, j = 1, 2, \ldots\}$, are orthogonal and may not be used as a basis to expand $h^{(2)}(\mathrm{x}, t)$. The reason is that an expansion such as $h^{(2)}(\mathrm{x}, t) = \sum h_{ij}^{(2)}(\mathrm{x}, t)\ (\xi_i\xi_j - \delta_{ij})$ will lead to $\langle h^{(2)}(\mathrm{x}, t)\rangle = 0$, because $\langle \xi_i\xi_j - \delta_{ij}\rangle = 0$. On the other hand, by taking the ensemble mean of Eqs. 22 through 26, we will find that $\langle h^{(2)}(\mathrm{x}, t)\rangle \neq 0$, unless the reservoir is homogeneous. We should also mention here that, in Ghanem and Spanos's algorithm (1991), the equations for different-order terms are coupled and cannot be solved separately, while in our algorithm, the equations for different-order terms of the pressure head are recursively defined (i.e., the equations for the higher-order terms depend on the lower-order terms, and equations with the same order are independent). As a result, all equations can be solved sequentially from lower order to higher order, and the equations with the same order can be solved in parallel. For example, after solving $h^{(0)}(\mathrm{x}, t)$ from Eqs. 7 through 10, we can solve for the first-order term $h_n^{(1)}(\mathbf{x}, t)$ from Eqs. 17 through 21. Note that the equations for $h_n^{(1)}(\mathbf{x}, t)$ with different n are independent and are thus inherently parallel, similar to the realizations in the Monte Carlo method.

It is very important to note that Eqs. 7, 17, and 22 have the same structure with the original flow equation (i.e., Eq. 1). In fact, Eq. 7, along with its corresponding initial and boundary conditions in Eqs. 8 through 10, is identical with the original flow Eq. 1 and its initial and boundary conditions in Eqs. 2 through 4 upon replacing K_s in the original equation by the geometric mean K_G. To obtain $h_n^{(1)}(\mathbf{x}, t)$, we only need to compute the boundary flux term in Eq. 20 and the source term $g_n^{(1)}(\mathbf{x}, t)$ in Eq. 21, and then solve Eq. 17 with initial and boundary conditions in Eqs. 18 through 20 using any flow solver. Higher-order pressure head terms can be solved in a similar manner (see Appendix). Treating the artificial source and sink terms in Eqs. 21 or 26 as equivalent wells at all nodes allows us to easily implement the KLME approach with the existing simulators, such as ECLIPSE, VIP, CHEARS, or other commonly used codes in the industry.

Computation of Pressure-Head Moments

To approximate the mean pressure head up to second order in σ_Y and the pressure-head covariance up to second order in σ_Y^2, we need to solve pressure head terms $h^{(0)}(\mathrm{x}, t)$, $h_i^{(1)}(\mathbf{x}, t)$, $h_{ij}^{(2)}(\mathbf{x}, t)$, and $h_{ijk}^{(3)}(\mathbf{x}, t)$. Once they are solved, we can directly calculate the mean pressure head and the pressure-head covariance (or any other higher-order moments) without solving the cross-covariance between the log hydraulic conductivity and the pressure head, which is required in the conventional moment-equation-based approach. Up to third order in σ_Y, the pressure head is approximated by

$$h(\mathbf{x}, t) \approx \sum_{m=0}^{3} h^{(m)}(\mathbf{x}, t), \quad (27)$$

which leads to an approximation for the mean pressure head

$$\langle h(\mathbf{x}, t)\rangle \approx h^{(0)}(\mathbf{x}, t) + \langle h^{(2)}(\mathbf{x}, t)\rangle = h^{(0)}(\mathbf{x}, t) + \sum_{i=1}^{\infty} h_{ii}^{(2)}(\mathbf{x}, t). \quad (28)$$

It is seen that $h^{(0)}(\mathrm{x}, t) = \langle h^{(0)}(\mathrm{x}, t)\rangle$ is the mean pressure-head solution up to first order in terms of σ_Y, and the second term on the right side of Eq. 28 represents the second-order (or third-order) correction to the 0th-order mean pressure head. From Eqs. 27 and 28, one can write an approximation for the pressure-head perturbation as

$$h'(\mathbf{x}, t) \approx h(\mathbf{x}, t) - \langle h(\mathbf{x}, t)\rangle = \sum_{m=1}^{3} h^{(m)}(\mathbf{x}, t) - \langle h^{(2)}(\mathbf{x}, t)\rangle. \quad (29)$$

From this equation, one derives the cross-covariance between the pressure head and the log hydraulic conductivity:

$$C_{Yh}(\mathbf{y}; \mathbf{x}, t) = \sum_{n=1}^{\infty} f_n(\mathbf{y}) h_n^{(1)}(\mathbf{x}, t) + \sum_{i,j=1}^{\infty} f_i(\mathbf{y}) h_{ijj}^{(3)}(\mathbf{x}, t), \quad (30)$$

and the pressure-head covariance:

$$C_h(\mathbf{x}, t; \mathbf{y}, \tau) = \sum_{n=1}^{\infty} h_n^{(1)}(\mathbf{x}, t) h_n^{(1)}(\mathbf{y}, \tau) = 2\sum_{i,j=1}^{\infty} h_{ij}^{(2)}(\mathbf{x}, t) h_{ij}^{(2)}(\mathbf{y}, \tau) + 3\sum_{i,j=1}^{\infty} h_i^{(1)}(\mathbf{x}, t) h_{ijj}^{(3)}(\mathbf{y}, \tau) + 3\sum_{i,j=1}^{\infty} h_i^{(1)}(\mathbf{y}, \tau) h_{ijj}^{(3)}(\mathbf{x}, t) \quad (31)$$

which leads to an expression for the pressure-head variance:

$$\sigma_h^2(\mathbf{x}, t) = \sum_{n=1}^{\infty}\left[h_n^{(1)}(\mathbf{x}, t)\right]^2 + 2\sum_{i,j=1}^{\infty}\left[h_{ij}^{(2)}(\mathbf{x}, t)\right]^2 + 6\sum_{i,j=1}^{\infty} h_i^{(1)}(\mathbf{x}, t) h_{ijj}^{(3)}(\mathbf{x}, t). \quad (32)$$

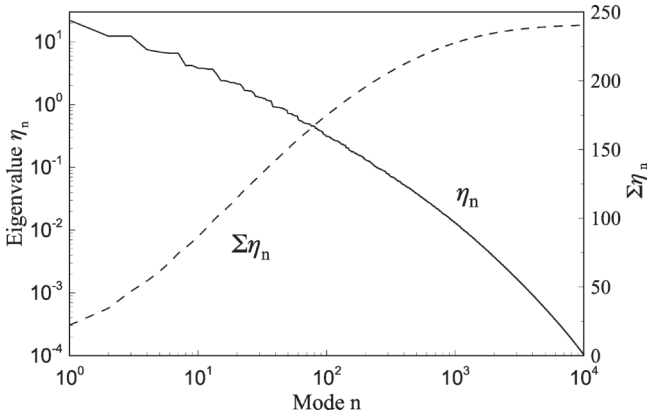

Fig. 1—The series of eigenvalues and their accumulative values.

The first summation in Eq. 32 stands for the first-order approximation (in σ_Y^2) of the pressure-head variance, and the remaining terms on the right side of Eq. 32 represent the second-order correction to the first-order pressure-head variance. Higher-order correction terms are given in Zhang and Lu (2004).

Illustrative Examples

In this section, we first attempt to examine the validity of the proposed KLME approach in computing high-order moments for transient fluid flow in hypothetical reservoirs by comparing model results with those from MCS. We then perform a large-scale simulation using the KLME method and compare the required computational effort with those of the Monte Carlo method and the conventional moment-equation method.

First we consider a 3D domain of a size $L_1 = L_2 = 8.0$ m and $L_3 = 4.0$ m in a hypothetical heterogeneous reservoir. The domain is uniformly discretized into 20×20×10 elements ($N = 4{,}851$ grid nodes in total). Initially, the pressure head in the entire domain is set to be 10.0 m. Starting at time $t = 0.0$, the pressure head is prescribed on the plane $\boldsymbol{x}_1 = 0.0$ m as $H_1 = 10.5$ m and on the plane $\boldsymbol{x}_1 = 8.0$ m as $H_2 = 10.0$ m, respectively. The no-flow conditions are prescribed on all other four surfaces. The statistics of the log hydraulic conductivity are given as $\langle Y \rangle = 0.0$ (i.e., the geometric mean of the hydraulic conductivity $K_G = 1.0$ m/day). For simplicity, it is assumed that the log hydraulic conductivity is second-order stationary and follows a separable exponential covariance function with a correlation length $\eta = 4.0$ m and variance $\sigma_Y^2 = 1.0$. In this case, the eigenvalues and eigenfunctions can be solved analytically (Zhang and Lu 2004). **Fig. 1** shows the eigenvalues as a function of mode number n for this case. It is seen that the eigenvalues are a nonincreasing series with respect to mode n. The accumulative eigenvalues are also illustrated in the figure. It is seen that the first 10 eigenvalues account for approximately 34% of the total variability and that the first 50 eigenvalues account for approximately 60% of the total variability. **Fig. 2** shows some examples of eigenfunctions f_n for the mode number $n = 1$, 5, 20, and 100. Note that the scale of the eigenfunction f_n decreases with the increase of the mode number n.

After solving for $h^{(0)}(\mathbf{x}, t)$, $h_i^{(1)}(\mathbf{x}, t)$, $h_{ij}^{(2)}(\mathbf{x}, t)$, and $h_{ijk}^{(3)}(\mathbf{x}, t)$, we then compute the mean pressure head up to second order in σ_Y using Eq. 28 and the pressure head variance up to second order in σ_Y^2 using Eq. 32.

For the purpose of comparison, we conducted MCS. We generated 2,000 3D realizations of the conductivity field, using Eq. 6 with the first 200 terms. The transient flow Eq. 1 with initial and boundary conditions from Eqs. 2 through 4 is solved for each realization of the conductivity field. Then, the sample statistics of the flow fields [i.e., the mean prediction of the pressure head as well as its associated uncertainty (pressure-head variance)] are

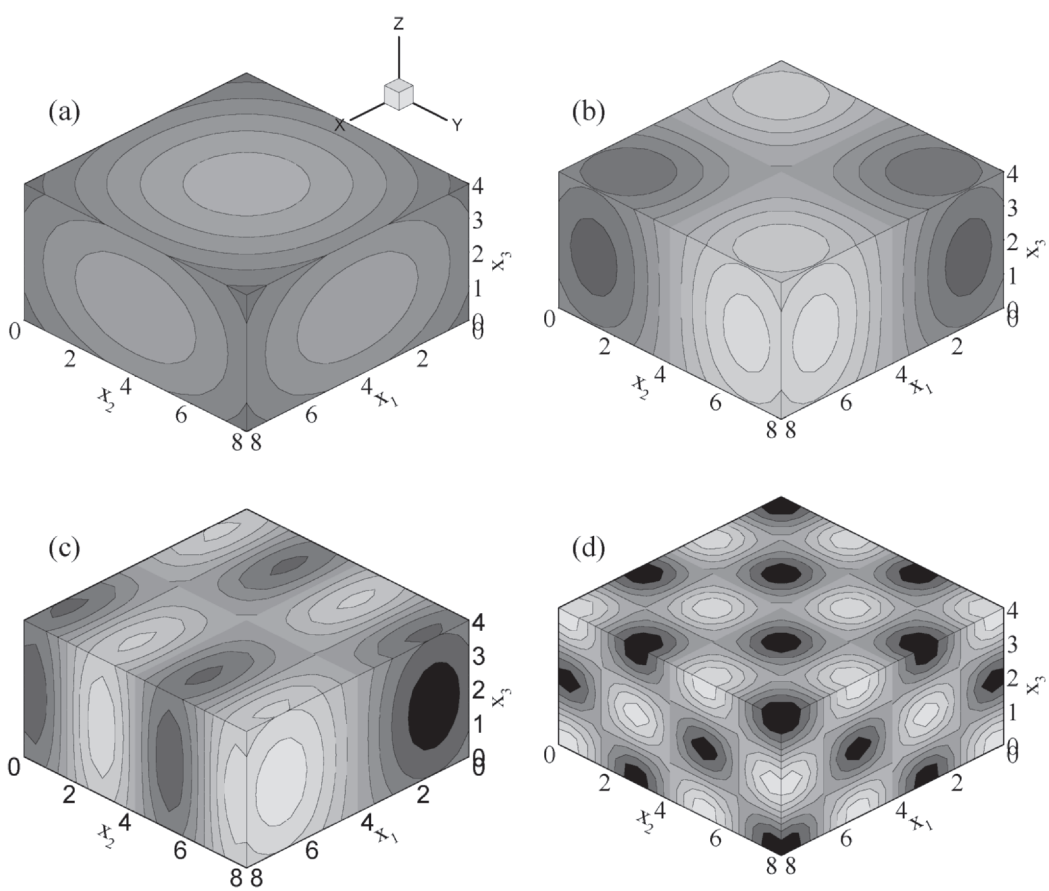

Fig. 2—Examples of eigenfunctions for the hypothetical reservoir: (a) $f_1(x)$; (b) $f_5(x)$; (c) $f_{20}(x)$; (d) $f_{100}(x)$.

computed from these realizations. These statistics are considered the "true" solutions, which are used to compare against the proposed high-order KLME approach.

First, we would like to investigate the efficiency and accuracy of the first-order KLME solutions. For this case (Case 1), we run steady-state simulations and approximate the first-order pressure-head moments with a different number of terms (n_1) included in the expansion of $h_n^{(1)}$, which is equivalent to taking only the first n_1 terms in approximating the pressure-head variance in Eq. 32.

Fig. 3 compares the mean pressure head and the pressure-head variance computed from MCS and from the KLME method up to the first order with $n_1 = 5$, 10, 20, and 50 terms, along the line that is the intersection of planes $\boldsymbol{x}_2 = 4.0$ m and $\boldsymbol{x}_3 = 2.0$ m. Because of the fact that $\langle h^{(1)}(\mathrm{x}, t)\rangle = 0$, the term $h_n^{(1)}$ does not make any contribution to the first-order mean pressure head. It is seen from the figure that the first-order KLME solution underestimates the pressure-head variance. We should emphasize that, although in the KL expansion of Y, $n_1 = 5$ terms only account for approximately 25% of the Y variability (see Fig. 1), the first-order approximation of the pressure-head variance using 5 terms is already in good agreement with that from the MCS. As the number of terms n_1 increases, the results are getting closer to the MCS result. For $n_1 = 50$, the pressure-head variance computed from the KLME approach is very close to the MCS result. The computational cost for obtaining the pressure-head variance with $n_1 = 50$ (circles in Fig. 3) is the cost of solving the set of linear algebraic equations with N unknowns for 51 times (once for the 0th-order mean pressure head $\langle h^{(0)}(\mathrm{x}, t)\rangle$), comparing to the cost of MCS. This is a substantial savings in computational efforts, not to mention that the numerical grid used in the KLME method could be much coarser than that in MCS.

It is of interest to investigate the accuracy of MCS with the same computational cost as compared to the KLME method. **Fig. 4** illustrates five sets of MCS, each of which includes 51 realizations. Certainly, MC results from the different sets of simulations are quite different, especially for the pressure-head variance. This implies that MCS with 51 realizations do not produce statistically meaningful results. A large number of realizations (such as 2,000 in this case) are needed to achieve converged statistics.

In the KL-based perturbation approach, instead of solving the covariance equations as in the conventional moment-equation method, we solve for the pressure-head terms $h_{i_1 i_2 \ldots i_m}^{(m)}$, which are given by linear algebraic equations with N unknowns. Once with the pressure-head terms, the first two moments of the pressure head can be obtained with simple algebraic operations. For the case of a grid of 21×21×11 mesh (i.e., 4,851 nodes) as in our examples, up to first-order, the conventional moment-equation approach requires to solve the moment equations on the grid for $2N = 9{,}702$ times, while the KL-based approach only needs to solve the pressure-head term equations for less than a hundred times on the same grid and to the same accuracy. Therefore, the KL-based perturbation approach is much more efficient than the conventional perturbation approach.

Two important factors may have contributed to the efficiency of this KL-based approach. First, the overall magnitudes of $h_{i_1,\ldots,i_m}^{(m)}$ decrease with order m for a small to moderate variability σ_Y^2. This allows us to use a relatively low order approximation under such a condition. In addition, for a fixed m, the magnitudes of $h_{i_1,\ldots,i_m}^{(m)}$ quickly approach 0 (statistically) as indices i_1, i_2, . . . , and i_m increase, which means that we can approximate $h^{(m)}$ with a relatively small number of terms. The magnitudes of the term $h_n^{(1)}$, $h_{ij}^{(2)}$, and $h_{ijk}^{(3)}$ are illustrated in **Fig. 5.** The figure shows that, in general, the higher-order terms are smaller in magnitude. For instance, for $\sigma_Y^2 = 1.0$, $h_n^{(1)}$ is in the order of 10^{-2}, while $h_{ij}^{(2)}$ is in the order of

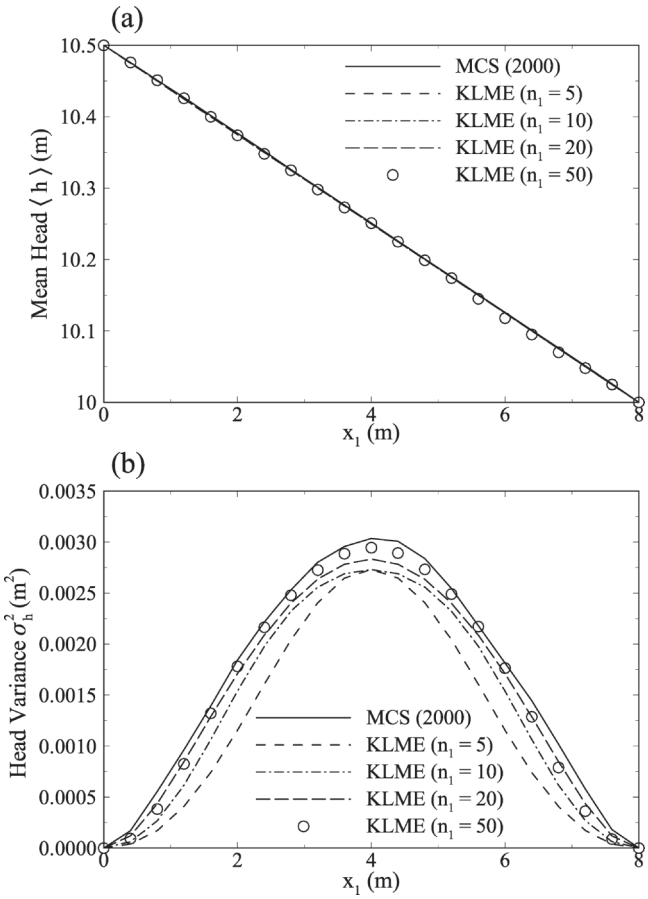

Fig. 3—Comparisons of (a) the mean pressure head, and (b) the pressure-head variance computed from MCS and the KLME method up to the first order with different number of terms in $h^{(1)}(x, t)$, for Case 1.

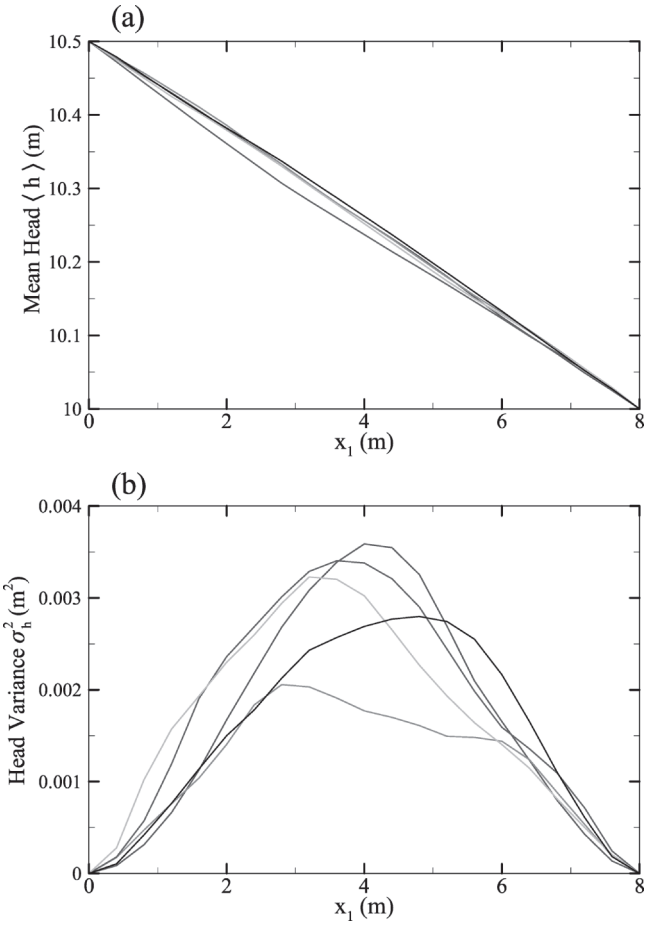

Fig. 4—(a) Mean pressure head and (b) pressure-head variance derived from five sets of MCS, each of which includes 51 realizations.

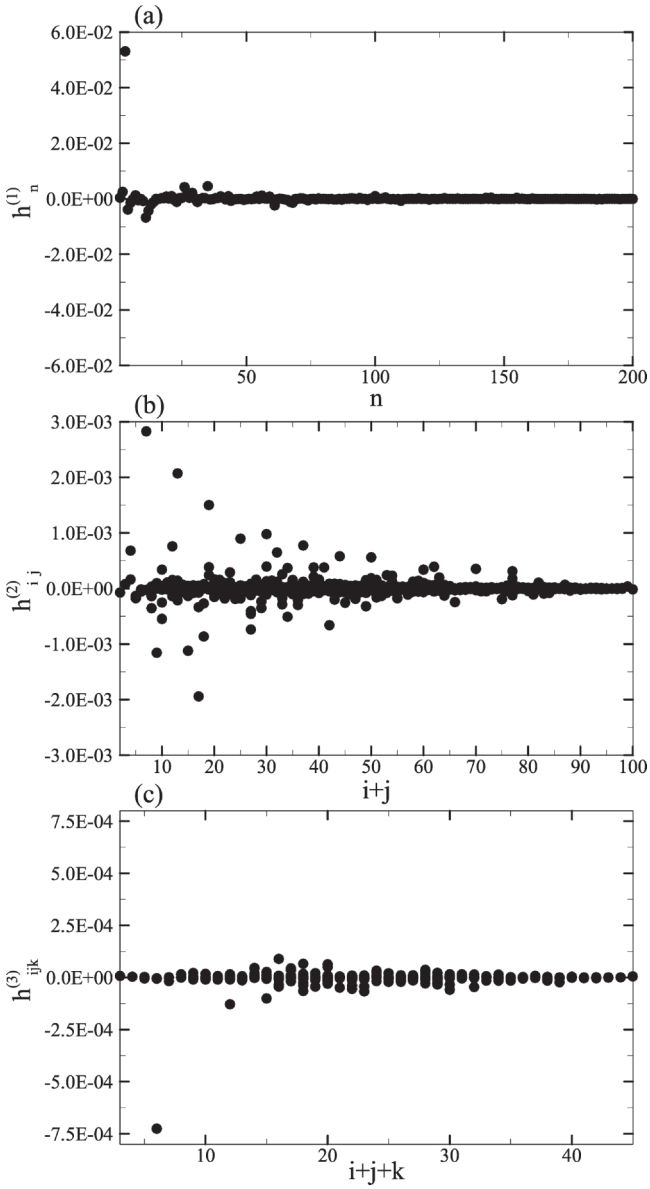

Fig. 5—Magnitude of pressure-head terms at the center of the domain: (a) First order, (b) second order, and (c) third order.

10^{-3}, and $h^{(3)}_{ijk}$ is in the order of 10^{-4}. It is also evident from the figure that $h^{(1)}_n$, $h^{(2)}_{ij}$, and $h^{(3)}_{ijk}$ decrease (statistically) as their indices become large.

In the previously described case, the first-order approximations are accurate enough. Higher-order corrections may be needed when the level of spatial variability increases (Zhang and Lu 2004; Li et al. 2003). In this study, we consider another situation in which the need for higher-order corrections stems from the flow configuration. In this case (Case 2), the same boundary conditions as Case 1 are specified, but the initial pressure head in the domain is assumed to be at steady state with a pressure head $H_1 = 10.5$ m on the plane $\boldsymbol{x}_1 = 0.0$ m and a pressure head $H_2 = 10.0$ m on the plane $\boldsymbol{x}_1 = 8.0$ m, respectively. Starting from $t = 0.0$, a pumping well of strength 20.0 m^3/d is placed in the center of the domain. **Fig. 6a** compares the steady-state mean pressure head derived from the MCS and from the KLME method up to second order in terms of σ_Y. It is seen that, in this case, there is a noticeable discrepancy between the mean pressure head computed from the MC results and the 0th-order mean pressure head from the KLME method, especially at the well location. By adding second-order corrections, the mean pressure head from the KLME method is getting closer to the Monte Carlo results. Fig. 6b compares the pressure-head variance computed from the MCS and from the

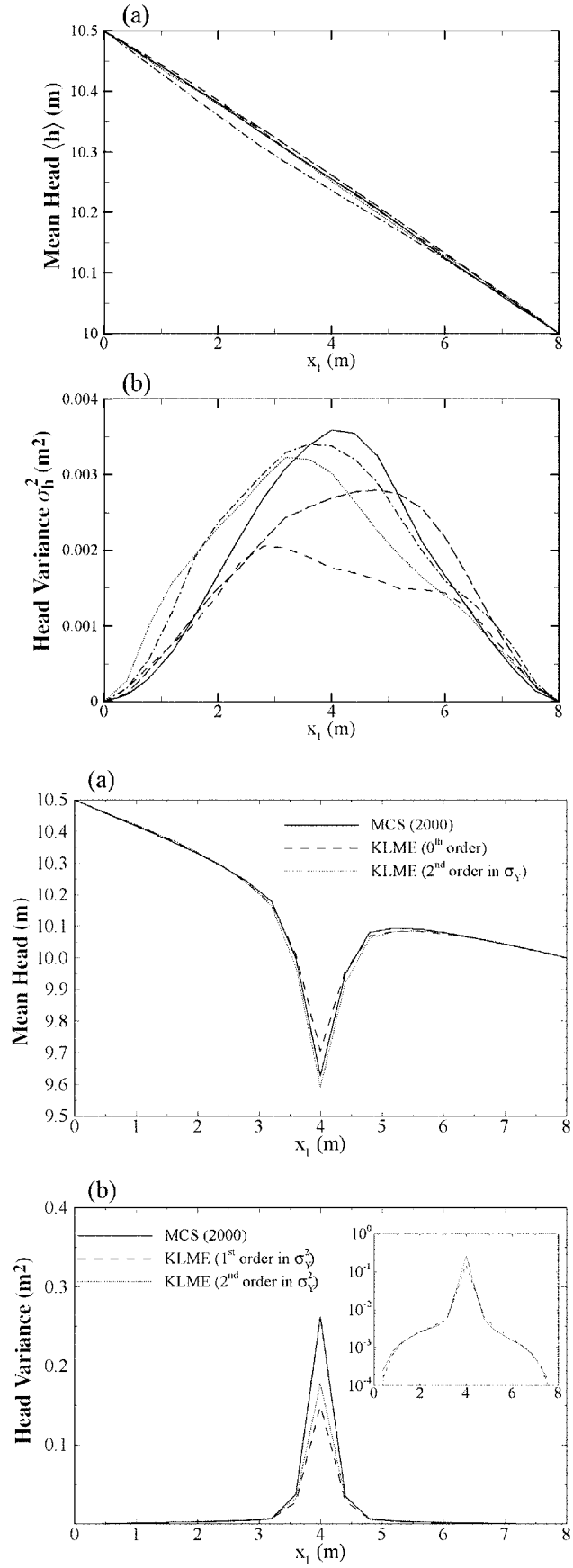

Fig. 6—Comparisons of (a) the mean pressure head, and (b) the pressure-head variance computed from MCS and the KLME method with the first- and second-order approximations (Case 2).

KLME method up to second order in terms of σ_Y^2. The figure shows that the second-order correction makes some improvement over the 0th-order results. Because the presence of the well significantly increases the head variability around the well locally, to better illustrate the comparison of the head variance away from the well, we plot the variance at the log scale, as shown in the insert of Fig. 6b. In this example, the number of terms included in approximating $h_n^{(1)}$, $h_{ij}^{(2)}$, and $h_{ijk}^{(3)}$ are, respectively, $n_1=100$, $n_2=30$, and $n_3=10$, which means that the term $h_n^{(1)}$ needs to be solved for 100 times, $h_{ij}^{(2)}$ for $30\times31/2=465$ times, and $h_{ijk}^{(3)}$ for $10\times11\times12/6=220$ times. The total number of times needed to solve the set of linear algebraic equations with 4,851 unknowns is $100+465+220=785$.

Case 3 is similar to Case 2, except that the flow is transient. **Fig. 7** compares the mean head and head variance computed from the MCS and the KLME method up to first-order approximations at three different times, $t=0.001$, 0.005, and 0.01 days. It is seen from the figure that the results from the KLME method are in good agreement with those from MCS, except at the well location. It should be noted that in the first-order KLME approach, we only solved Eqs. 17 through 20 for 100 times, as compared to solving Eqs. 1 through 4 for 2,000 times in the MC approach.

Finally, we consider a more realistic large-scale problem of 3D flow (Case 4) with $L_1=L_2=10000$ m and $L_3=500$ m in a hypothetical heterogeneous reservoir. The domain is uniformly discretized into elements of size 125×125×12.5 m ($N=269{,}001$ nodes in the numerical grid). Initially, the pressure-head distribution in the entire domain is at steady state with a constant pressure head on the plane $\boldsymbol{x}_1=0.0$ m as $H_1=110$ m and on the plane $\boldsymbol{x}_1=10\,000$ m as $H_2=100.0$ m. All other boundaries are no-flow boundaries. Starting at time $t=0.0$, a pumping well with a strength of 0.01/d is placed at the center of the domain (node 135,001). It is assumed that the reservoir is statistically homogeneous and the mean of the log hydraulic conductivity is given as $\langle Y\rangle=0.0$. For simplicity, it is also assumed that the covariance of the log hydraulic conductivity is a separable anisotropic exponential function with variance $\sigma_Y^2=1.0$ and correlation lengths $\eta_1=\eta_2=500$ m and $\eta_3=50$ m. **Fig. 8** shows a single realization of the log saturated hydraulic conductivity. For such a large-scale problem, each transient simulation will take hours of computational time. As a result, the MC method is very time-consuming, because a large number of MC realizations are needed to achieve statistical convergence. As illustrated in Fig. 4, a small number of MCS will not give any statistically meaningful results. The conventional moment method is almost infeasible for this case for two reasons. First, even for the first-order head variance, it requires solving sets of linear algebraic equations with 269,001 unknowns for approximately $2N=538{,}002$ times. In addition, the conventional moment method needs to store the cross-covariance function C_{Yh}, which is an asymmetric matrix of a size 269,001×269,001, requiring over 578 GB of memory. In the KLME approach, we only have to solve the linear algebraic equations on the grid of 269,001 nodes for a small number of times (n_1). **Fig. 9** depicts the first-order steady-state mean pressure head and the pressure-head variance computed using KLME method for $n_1=50$.

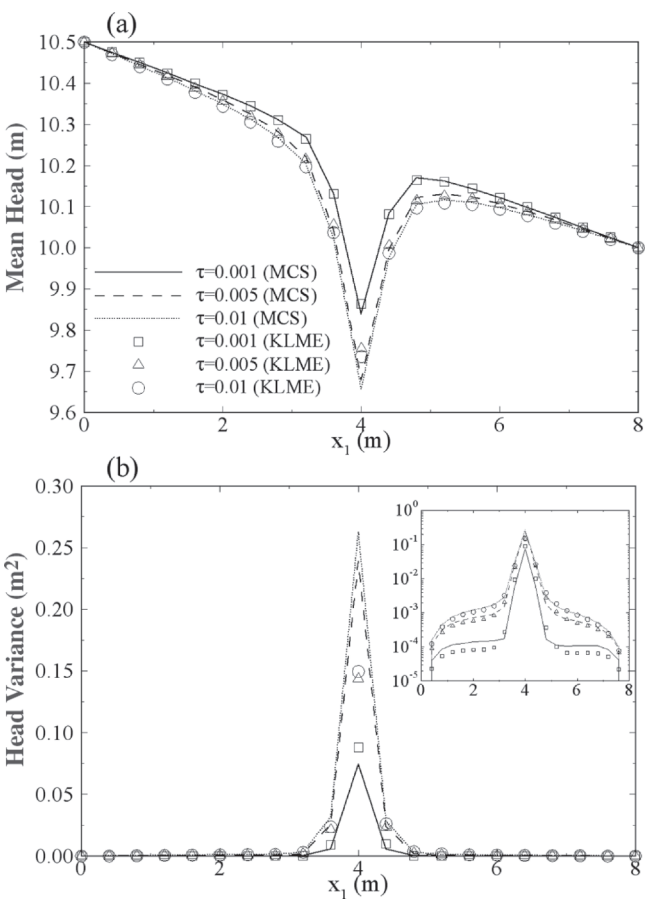

Fig. 7—Comparisons of (a) the mean pressure head, and (b) the pressure-head variance computed from MCS and the KLME method with the first-order approximation at different elapsed times (Case 3).

Summary and Conclusions

In this study, we combined the moment-equation approach with the KL and polynomial expansions to evaluate the statistical moments of fluid flow in randomly heterogeneous reservoirs. We first decomposed the log hydraulic conductivity into an infinite series related to the eigenvalues and eigenfunctions of the covariance function of log hydraulic conductivity as well as a set of standard Gaussian random variables. We then decomposed the pressure head into a series whose terms $h^{(m)}$ are mth order in terms of σ_Y. By further assuming that $h^{(m)}$ can be expanded into a series in terms of the product of m Gaussian random variables, we arrived at sets of equations for determining the deterministic coefficients in these expansions. Once these coefficients are solved, the mean pressure head and the pressure-head covariance can be computed easily. This study leads to the following conclusions:

1. The moment-equation approach based on KLME makes it possible to evaluate higher-order moments with relatively small computational efforts.
2. In this algorithm, the equations for different-order pressure head terms are recursively defined (i.e., the equations for the higher-order terms depend on the lower-order terms, and equations with the same order are independent). As a result, all equations can be solved sequentially from lower to higher-order.
3. At the same order, the equations are independent. These equations, like the realizations in the MC method, are inherently parallel and are thus amenable to parallel computation.

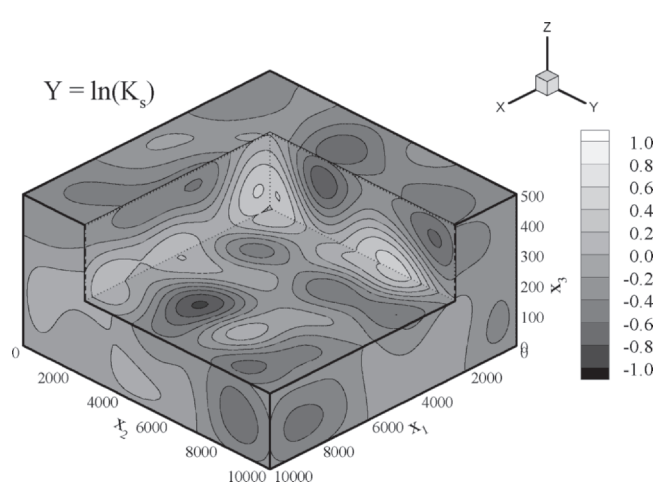

Fig. 8—A realization of the log hydraulic conductivity field (the dimension in the vertical direction is exaggerated).

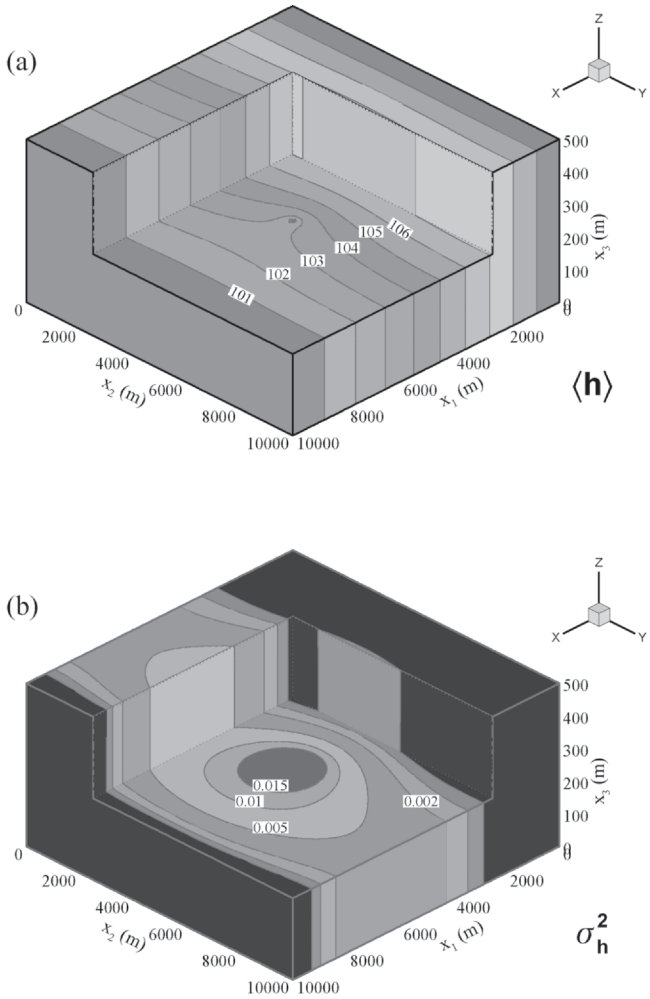

Fig. 9—Contour maps of the first-order (a) mean pressure head and (b) pressure-head variance computed from the KLME method for the large-scale problem (Case 4).

4. The KL-based moment equations have the same structure, as does the original flow equation. For this reason, similar to the MCS method, the KLME approach can be easily implemented with the existing simulators, such as ECLIPSE, VIP, CHEARS, or other commonly used codes in the industry.
5. The KLME approach is computationally more efficient than both the MCS and the conventional moment-equation method. Although the governing equations are similar for the realizations of the MCS method and for the coefficients of the pressure-head term in the KLME approach, the underlying randomness of the log hydraulic conductivity is treated differently. In the former, equally likely realizations are generated such that a large number of realizations are needed to achieve convergent statistics; in the latter, the modes of the random field are ranked and ordered by the eigenvalues and eigenfunctions so that the random field may be largely captured with a limited number of dominant modes. The KLME approach is more efficient than the conventional moment-equation method, because the former avoids solving the full covariance equations of size N^2 but constructs the needed covariances from the coefficients of size N (where N is the number of grid nodes).
6. The KLME approach is particularly suitable for the problem of uncertainty quantification for fluid flow in large-scale heterogeneous reservoirs.

The current version of the KLME model is limited to Gaussian random fields. However, it could be extended to non-Gaussian fields. There are two possible approaches to attack this problem. One is to expand the non-Gaussian field using the KL decomposition and then apply the KLME method to the problem, because the input to our equations are the KL expansions, no matter how these expansions are obtained. Another promising approach is to consider dividing the flow domain into different zones in such a way that the random function (say, permeability) in each of these zones is Gaussian.

Nomenclature

C_h = covariance of head h, L^2
C_{Yh} = cross-covariance between Y and head h
D = simulation domain
f_n = eigenfunctions (–)
g = source/sink term, T^{-1}
h = hydraulic pressure head, L
$h^{(m)}_{i_1 i_2 \ldots i_m}$ = mth-order terms
H = prescribed head on Dirichlet boundary, L
H_0 = initial pressure head in the flow domain, L
K_G = geometric mean of hydraulic conductivity, LT^{-1}
K_s = hydraulic conductivity, LT^{-1}
L_i = dimension in ith direction
$\boldsymbol{n}$ = an outward unit vector normal to boundaries
n_i = number of terms used in ith-order approximation
N = number of grid nodes (–)
Q = flux across Neumann boundary segments, LT^{-1}
S_s = specific storage, L^{-1}
t = time, T
V = volume of the simulation domain
$\mathbf{x}$ = Cartesian coordinate, L
Y = log hydraulic conductivity (–)
Γ_D = Dirichlet boundary segments
Γ_N = Neumann boundary segments
η = correlation length, L
λ_n = eigenvalues
ξ_i = orthogonal random variables (–)
σ_Y^2 = variance of the log hydraulic conductivity (–)

Acknowledgments

This work was partially supported by the Los Alamos Natl. Laboratory through its LDRD/DR project "Science of Geological Carbon Sequestration," by American Chemical Society through its Petroleum Research Fund (Grant #42109-AC9), and by Chinese Natural Science Foundation through its Grant 50310444.

References

Chen, M., Zhang, D., Keller, A.A., and Lu, Z. 2005. A stochastic analysis of steady state two-phase flow in heterogeneous media. *Water Resour. Res.* **41** W01006, doi:10.1029/2004WR003412.

Dagan, G. 1989. *Flow and Transport in Porous Formations.* Springer: New York City.

Gelhar, L.W. 1993. *Stochastic Subsurface Hydrology*. Prentice-Hall: Englewood Cliffs, New Jersey.

Ghanem R. and Spanos, P.D. 1991. *Stochastic Finite Elements: A Spectral Approach*. Springer-Verlag: New York City.

Li, L. and Tchelepi, H.A. 2003. Conditional Stochastic Moment Equations for Uncertainty Analysis of Flow in Heterogeneous Reservoirs. *SPEJ.* **8** (4): 392–400. SPE-79675-PA.

Li, L., Tchelepi, H.A., and Zhang, D. 2003. Perturbation-Based Stochastic Moment Equation Approaches: Applicability Range, Analysis of High-Order Terms, and Consistency With Monte Carlo Simulation. *Journal of Computational Physics* **188:** 296–317.

Lu, Z. and Zhang, D. 2004a. Conditional simulations of flow in randomly heterogeneous porous media using a KL-based moment-equation approach. *Advances in Water Resour.* **27** (9): 859–874.

Lu, Z. and Zhang, D. 2004b. A comparative study on quantifying uncertainty of flow in heterogeneous media using Monte Carlo simulations, the conventional and the KL-based moment-equation approaches. *SIAM J. Scientific Computing* **26** (2): 558–577.

Roy, R.V. and Grilli, S.T. 1997. Probabilistic analysis of the flow in random porous media by stochastic boundary elements. *Engrg. Analysis with Boundary Elements* **19:** 239–255.

Yang, J., Zhang, D., and Lu, Z. 2004. Stochastic analysis of saturated-unsaturated flow in heterogeneous media by combining Karhunen-Loeve expansion and perturbation method. *J. Hydrol.* **294:** 18–38.

Zhang, D. 2002. *Stochastic Methods for Flow in Porous Media: Coping with Uncertainties*. Academic Press: San Diego, California.

Zhang, D. and Lu, Z. 2004. An efficient, higher-order perturbation approach for flow in randomly heterogeneous porous media via Karhunen-Loeve decomposition. *J. Comput. Physics* **194** (2): 773–794.

Appendix

In the KLME approach, we further expand the mth-order pressure-head terms $h^{(m)}$ as the mth polynomial function of the set of Gaussian random variances ξ_n:

$$h^{(m)}(\mathbf{x}, t) = \sum_{i_1, i_2, \ldots, i_m = 1}^{\infty} \left(\prod_{j=1}^{m} \xi_{i_j} \right) h^{(m)}_{i_1, i_2, \ldots, i_m}(\mathbf{x}, t), \quad \text{(A-1)}$$

where $h^{(m)}_{i_1 i_2 \ldots i_m}$ are deterministic functions to be solved. Substituting the decomposition of $Y'(\mathbf{x})$ and $h^{(m)}$ recursively Eqs. 11 through 15, we obtain the governing equations for $h^{(m)}_{i_1 i_2 \ldots i_m}$:

$$\nabla \cdot [K_G(\mathbf{x}) \nabla h^{(m)}_{i_1, i_2, \ldots, i_m}(\mathbf{x}, t)] + g^{(m)}_{i_1, i_2, \ldots, i_m}(\mathbf{x}, t) = S_s \frac{\partial h^{(m)}_{i_{k+1}, \ldots, i_m}(\mathbf{x}, t)}{\partial t} \quad \text{(A-2)}$$

subject to the initial and boundary conditions

$$h^{(m)}_{i_1, i_2, \ldots, i_m}(\mathbf{x}, 0) = 0, \qquad \mathbf{x} \in D, \quad \text{(A-3)}$$

$$h^{(m)}_{i_1, i_2, \ldots, i_m}(\mathbf{x}, t) = 0, \qquad \mathbf{x} \in \Gamma_D, \quad \text{(A-4)}$$

$$K_G(\mathbf{x}) \nabla h^{(m)}_{i_1, i_2, \ldots, i_m}(\mathbf{x}, t) \cdot \mathrm{n}(\mathbf{x}) = \frac{(-1)^{m+1} Q(\mathbf{x}, t)}{m!} \prod_{j=1}^{m} f_{i_j}, \qquad \mathbf{x} \in \Gamma_N, \quad \text{(A-5)}$$

where

$$g^{(m)}_{i_1, \ldots, i_m}(\mathbf{x}, t) = \frac{K_G(\mathbf{x})}{m} \sum_{P_{i_1, \ldots, i_m}} \nabla f_{i_1}(\mathbf{x}) \cdot \nabla h^{(m-1)}_{i_1, \ldots, i_m}(\mathbf{x}, t) + \frac{(-1)^m g(\mathbf{x}, t)}{m!} \left(\prod_{j=1}^{m} f_{i_j} \right) - S_s \sum_{k=1}^{m} \frac{(-1)^k (m-k)!}{m!} \sum_{P_{i_1, \ldots, i_m}} \left(\prod_{j=1}^{k} f_{i_j} \right) \frac{\partial h^{(m-k)}_{i_{k+1}, \ldots, i_m}(\mathbf{x}, t)}{\partial t} \quad \text{(A-6)}$$

Here, the summation in Eq. A-6 is over a subset of the permutation of the set $\{i_1, i_2, \ldots, i_m\}$, in which repeated terms are excluded. For instance, $\sum_{P_{ijk}} \nabla f_i \cdot \nabla h^{(2)}_{jk} = \nabla f_i \cdot \nabla h^{(2)}_{jk} + \nabla f_j \cdot \nabla h^{(2)}_{ik} + \nabla f_k \cdot \nabla h^{(2)}_{ij}$. The rest of terms, such as $\nabla f_i \cdot \nabla h^{(2)}_{kj}$, which is the same as $\nabla f_i \cdot \nabla h^{(2)}_{jk}$, are not included. By doing so, we ensure that $h^{(m)}_{i_1 i_2 \ldots i_m}$ is symmetric with its indices in subscripts. Because of symmetry of term $h^{(m)}_{i_1, \ldots, i_m}$ with respect to its indices (subscripts), to obtain $h^{(m)}_{i_1, \ldots, i_m}$, where i_j runs from 1 to some given number n, the number of times required to solve Eqs. A-2 through A-5 is $S_m = n(n+1) \cdots (n+m-1)/m!$. For example, for $n = 20$, we need to solve $h^{(2)}_{ij}$ for $S_2 = 20 \times 21/2 = 210$ times.

The equations and their corresponding initial and boundary conditions for $h^{(1)}_n$ and $h^{(2)}_{ij}$ are given in Eqs. 17 through 21 and 22 through 26. For the third-order terms $h^{(3)}_{ijk}$, the equation reads

$$\nabla \cdot [K_G(\mathbf{x}) \nabla h^{(3)}_{ijk}(\mathbf{x}, t)] + g^{(3)}_{ijk}(\mathbf{x}, t) = S_s \frac{\partial h^{(3)}_{ijk}(\mathbf{x}, t)}{\partial t} \quad \text{(A-7)}$$

subject to the initial and boundary conditions

$$h^{(3)}_{ijk}(\mathbf{x}, 0) = 0, \qquad \mathbf{x} \in D, \quad \text{(A-8)}$$

$$h^{(3)}_{ijk}(\mathbf{x}, t) = 0, \qquad \mathbf{x} \in \Gamma_D, \quad \text{(A-9)}$$

$$K_G(\mathbf{x}) \nabla h^{(3)}_{ijk}(\mathbf{x}, t) \cdot \mathbf{n}(\mathbf{x}) = \frac{Q(\mathbf{x}, t)}{6} f_i(\mathbf{x}) f_j(\mathbf{x}) f_k(\mathbf{x}), \qquad \mathbf{x} \in \Gamma_N, \quad \text{(A-10)}$$

where

$$g^{(3)}_{ijk}(\mathbf{x}, t) = \frac{K_G(\mathbf{x})}{3} \sum_{P_{ijk}} \nabla f_i(\mathbf{x}) \cdot \nabla h^{(2)}_{jk}(\mathbf{x}, t) - \frac{g(\mathbf{x}, t)}{6} f_i(\mathbf{x}) f_j(\mathbf{x}) f_k(\mathbf{x}) + \frac{S_s}{6} \sum_{P_{ijk}} \left[2 f_i(\mathbf{x}) \frac{\partial h^{(2)}_{jk}(\mathbf{x}, t)}{\partial t} - f_i(\mathbf{x}) f_j(\mathbf{x}) \frac{\partial h^{(1)}_k(\mathbf{x}, t)}{\partial t} + f_i(\mathbf{x}) f_j(\mathbf{x}) f_k(\mathbf{x}) \frac{\partial h^{(0)}(\mathbf{x}, t)}{\partial t} \right] \quad \text{(A-11)}$$

Zhiming Lu is a technical staff member in the Earth and Environmental Sciences Div. at the Los Alamos Natl. Laboratory. e-mail: zhiming@lanl.gov. His research interests include quantifying uncertainty for flow and transport in randomly heterogeneous porous media and inverse modeling. He holds a BS degree in applied mathematics from Zhejiang U., China, an MS degree in applied earth sciences from Stanford U., and a PhD degree in hydrology from the U. of Arizona. **Dongxiao Zhang** is the Miller Chair Professor in Petroleum and Geological Engineering at the U. of Oklahoma, where he has been a faculty member since 2004. From 1996 to 2003, he was a technical staff member and a team leader at the Los Alamos Natl. Laboratory. His research interests include stochastic uncertainty quantification of reservoir simualtions, pore-scale processes, and geological carbon sequestration. Zhang holds MS and PhD degrees in hydrology from the U. of Arizona.